Retrieval of Profile Information from Airborne Multi Axis UV/visible Skylight Absorption Measurements

Marco Bruns[1], Stefan A. Buehler[1], John P. Burrows[1], Klaus-Peter Heue[2], Ulrich Platt[2], Irene Pundt[2], Andreas Richter[1], Alexej Rozanov[1], Thomas Wagner[2], Ping Wang[1]

[1]*Institute of Environmental Physics, University of Bremen, P.O. Box 33 04 40, 28359 Bremen, Germany and*

[2]*Institute of Environmental Physics, University of Heidelberg, Im Neuenheimer Feld 229, 69120 Heidelberg, Germany*

Abstract

A recent development in ground-based remote sensing of atmospheric constituents by UV/visible absorption measurements of scattered light is the simultaneous use of several horizon viewing directions in addition to the traditional zenith-sky pointing. The different light paths through the atmosphere enable the vertical distribution of some atmospheric absorbers such as NO_2, BrO or O_3 to be retrieved. This approach has recently been implemented on an airborne platform. The novel instrument called Airborne MultiAXis Differential Optical Absorption Spectrometer, AMAX-DOAS, has been flown for the first time.

In this study, the amount of profile information that can be retrieved from such measurements is investigated. Sensitivity studies of synthetic data were performed for a variety of representative measurement conditions including two wavelengths, one in the UV and one in the visible, two different surface spectral reflectance, various lines of sight (LOS), and for two different flight altitudes.

The results demonstrate that the AMAX-DOAS measurements contain useful profile information, mainly at flight altitude and below the aircraft. Depending on wavelength and LOS used, the vertical resolution of the retrieved profiles is 2 km up to an altitude of approximately 14 km. Above 14 km the profile information content of AMAX-DOAS measurements is sparse. Airborne multiaxis measurements are thus a promising tool for atmospheric studies in the troposphere and the UTLS region.

OCIS codes: 000.3860, 010.1290, 010.1310, 010.7030, 280.1120, 300.6540.

1. Introduction

Since the early 1970's ground-based measurements of the ultraviolet and visible light scattered from the zenith sky have been used to determine the absorptions and thereby derive the atmospheric column densities of various trace gases (e.g. O_3, NO_2, BrO, OClO, ...) by several research groups e.g.[1–5]. These measurements identify specific absorption features using the well known Differential Optical Absorption Spectroscopy (DOAS) method[6]. The typical quantity derived from such measurements is a differential slant column density, that is the difference of the integrated column of molecules along the different light paths through the atmosphere. This is converted to a vertical column by a so-called air mass factor.

A scientifically more interesting quantity is the atmospheric profile of a trace gas. Noxon et. al.[7] were the first to estimate the profile information contained in slant column measurements. Later McKenzi et. al.[8] used the weighted Chahine inversion, an iterative method that requires a convergence constraint to retrieve vertical NO_2 profiles. Preston et. al.[9,10] used the Optimal Estimation method to retrieve NO_2 profiles from ground-based UV/visible zenith skylight absorption measurements at different SZA. The vertical resolution of such profiles is relatively low, and up to now profile retrievals were only attempted for NO_2. Vertically resolved measurements would also be of interest for BrO to investigate the presence of BrO in the boundary layer and in the free troposphere and its role in catalytic cycles removing O_3[11–17].

Airborne UV/visible zenith sky absorption measurements have been performed since the 1980's[18–26]. The experimental setups in these works apply zenith sky absorption measurements to retrieve trace gas columns. More recently, Petritoli et. al.[27] have demonstrated that by using an horizon pointing (off-axis) measurement, the retrieval of in-situ information near flight altitude is possible.

For the validation of measurements from the SCIAMACHY[39] instrument on board of ENVISAT, the Airborne MultiAxis DOAS instrument (AMAX-DOAS)[28] was developed, that takes simultaneous measurements of UV/visible sky absorptions at different lines of sight (LOS) pointing above and below the aircraft. The main focus of the AMAX-DOAS measurements is the retrieval of stratospheric and tropospheric columns by using the zenith-sky and nadir viewing directions at a flight altitude close to the tropopause. However, the additional viewing directions were added to investigate the possibility to derive information on the vertical distribution of the absorbers. This is similar to the approach used in ground-based multiaxis measurements[29,30], which resolves the lower troposphere. More independent pieces of information are expected for AMAX-DOAS as compared to the ground-based multiaxis DOAS, as a result of the viewing geometry observed from an aircraft.

It should be noted that the geometry, used in these studies (several LOS measured at one SZA), differs from that used in previous profiling studies, where measurements at one LOS but various SZA were performed, and the variation of scattering height as a function of SZA is used to extract the profile information from the measurements as shown by Preston et. al.[9,10]. In this study, the information content of airborne multiaxis measurements is evaluated, and sensitivity studies are performed to assess the impact of different parameters on the retrieved profiles. A best case scenario with cloudless clear skies and simplified measurement errors is used. The results of this study provide an upper estimate of profile information, which can be retrieved from real measurements. The study is intended for the analysis of measurements from the AMAX-DOAS instrument, but the results are also valid for other airborne DOAS measurements.

2. The Measurement Geometry

Before discussing the retrieval theory and the sensitivity study, a qualitative discussion of the viewing geometry highlights and explains the concept to be exploited by the multiaxis measurements. Fig. 1 a.) shows the measurement geometry of AMAX-DOAS measurements assuming single-scattering. The ray coming directly from the sun penetrates the atmosphere and is scattered at a specific altitude. As can be seen in this plot, the light paths after scattering are different, and depend on the LOS. This feature is used by the method described below to retrieve profile information by combining simultaneous measurements of different directions. The distance of the point of scattering from the aircraft is determined by the visibility. The visibility depends on the wavelength, the density of the atmosphere, the aerosol loading, and in the case of nadir view also the distance to the surface.

The upward looking LOS all see the atmosphere above the aircraft, but in the single-scattering approximation are not influenced by the atmosphere below flight altitude. The height from which most of the measurement signal originates depends strongly on the length it travels through denser areas of the atmosphere close to the aircraft. Therefore LOS pointing near the horizon will retrieve a relatively larger signal from the altitudes near flight altitude than LOS pointing more to the zenith.

All downward looking LOS do see the atmosphere above the aircraft too but in addition also probe the atmosphere below flight altitude. These LOS can be divided into two categories. The first category is for those LOS where radiation is scattered above the earth's surface. We call these LOS the limb mode of the AMAX-DOAS instrument. For such LOS the largest part of the measurement signal is coming from the tangent height. The different tangent heights for different LOS yield the profile information in the measurements. The tangent height is the lowest altitude the LOS penetrate due to the spherical shape of the earth.

For the single scattering approximation such LOS do not see the atmosphere below that altitude. The second category of LOS include those viewing directions where radiation is scattered close to or at the earth's surface. We call these LOS the nadir mode of the AMAX-DOAS instrument. As all these LOS probe all altitudes below the aircraft, the information content of the profile is small and only based on different amounts of scattering depending on the viewing angle. In general these explanations are valid for both the visible and the UV wavelength regions. In the UV the larger extinction by Rayleigh scattering reduces the visibility. These LOS will then act as limb LOS and potentially add profile information below the aircraft.

The radiative modeling used in the quantitative studies reported below includes full multiple scattering and is not limited to the simple assumptions made here.

3. The Retrieval Method

The profile retrieval method used in this work is based on Preston et. al.[9,10]. The retrieval method was modified for the application to airborne UV-visible absorption measurements. The modified method retrieves the profile information using various lines of sight at the same solar zenith angle, whereas the original method retrieves the profile information using only one line of sight but various solar zenith angles [see Fig. 1 b.)].

This retrieval method requires a forward model to calculate the measurement quantity. In the case of DOAS retrievals these are not the radiances but the slant columns for a given trace gas vertical profile. For the simulation of the slant columns, the radiative transfer model SCIATRAN[34] was used. SCIATRAN is a full spherical radiative transfer model taking into account refraction and multiple scattering. It is able to calculate the radiance in specific lines of sight for a specific flight altitude. The radiances produced by the radiative transfer model are used to calculate air mass factors:

$$AMF(\lambda, j) = \frac{1}{VOD(\lambda, j)} \ln\left(\frac{I(\lambda, gas\ j = OFF)}{I(\lambda, gas\ j = ON)}\right) \quad (1)$$

VOD(λ, j) is the vertical optical depth of trace gas j at wavelength λ, I(λ, where gas j = off) is the intensity (radiance) at wavelength λ without trace gas j, and I(λ, gas j = on) is the intensity (radiance) at wavelength λ with trace gas j.

The vertical columns (VC) are converted into simulated slant columns (SC) using the air mass factors of eq. (1).

$$AMF = \frac{SC}{VC} \quad (2)$$

In the sensitivity studies, the SC has been computed using one AMF representative of the spectral window. While this might not always be appropriate for the retrieval of real data, it does not introduce any uncertainties in self-consistent model studies as those discussed here.

4. The Retrieval Theory

A set of slant columns at a certain SZA using different LOS contains information about the vertical distribution of a specific trace gas in the atmosphere. To analyze the quality of the information for profile retrieval the characterization of a retrieval method from Rodgers[31–33] is used. This characterization includes a formal treatment of errors. A set of measurements **y** can be related to a vertical profile **x** by a forward model F[32].

$$\mathbf{y} = F(\mathbf{x},\mathbf{b}) + \epsilon \quad (3)$$

where **b** is the vector of the forward model parameters and ϵ is the error of the measurement. The error ϵ consists of different error components, which are discussed in the error analysis

section. In our case, $\mathbf{y}$ is a vector of slant columns as a function of LOS, and $\mathbf{x}$ is the vertical profile of the trace gas of interest. The profile $\mathbf{x}$ - a continuous function in the real atmosphere - has to be sampled discretely by the retrieval algorithm and is therefore presented as a vector. Eq. 3 can be rewritten in a linearized form[31]:

$$\Delta\mathbf{y} = \mathbf{K}\Delta\mathbf{x} \tag{4}$$

where

$$\mathbf{K} = \frac{d\mathbf{y}}{d\mathbf{x}} \tag{5}$$

The rows of the $\mathbf{K}$ matrix represent the weighting functions, and each row corresponds to a different measurement. Each LOS is considered as a single measurement. The weighting functions describing this problem contain the dependence of the slant columns on the vertical profile for each LOS. In other words: the weighting functions give the change of the slant column when varying the VMR of the profile by a certain amount at a certain altitude.

There is no unique solution to the inversion of eq. 4, because the problem is ill-posed with a condition-number κ. The latter is calculated by doing a singular value decomposition of matrix $\mathbf{K}$. κ is the ratio of the largest and the smallest singular values. A large value κ in the range of 10^6 or larger means the problem is ill-conditioned. In the case of scenario 1 (see Tab. 1 for a description of scenario 1) κ is in the order of 10^{29}. To reduce the amount of possible solutions the Optimal Estimation Method described by Rodgers[31–33] adds a priori information. A requirement for the Optimal Estimation method to be used is linearity of the problem. The retrieval problem for trace gas skylight absorption measurements is essentially linear because most trace gases (e.g. NO_2) are optically thin (i.e. absorptions smaller than 2%). In this study the Maximum a Posteriori (MAP) solution was chosen[33]. This method

calculates the retrieved profile as follows:

$$\hat{\mathbf{x}} = \left(\mathbf{K}^T\mathbf{S}_\epsilon^{-1}\mathbf{K} + \mathbf{S}_a^{-1}\right)^{-1}\left(\mathbf{K}^T\mathbf{S}_\epsilon^{-1}\mathbf{y} + \mathbf{S}_a^{-1}\mathbf{x}_a\right) \tag{6}$$

where $\mathbf{K}$ is the weighting function matrix, $\mathbf{S}_\epsilon$ is measurement error covariance matrix, $\mathbf{S}_a$ is the arbitrary error covariance matrix of the a priori information, $\mathbf{y}$ is the measurement vector, and $\mathbf{x}_a$ is the a priori profile information.

To characterize the retrieved profile more precisely, the contribution function matrix $\mathbf{D}$ is introduced. This represents the sensitivity of the retrieved profile to the changes of the slant columns:

$$\mathbf{D} = \frac{\partial\hat{\mathbf{x}}}{\partial\mathbf{y}} = \mathbf{S}_a\mathbf{K}^T\left(\mathbf{K}\mathbf{S}_a\mathbf{K}^T + \mathbf{S}_\epsilon\right)^{-1} \tag{7}$$

where $\mathbf{S}_a$ is the arbitrary error covariance matrix of the a priori information, $\mathbf{K}^T$ is the transposed weighting function matrix $\mathbf{K}$, and $\mathbf{S}_\epsilon$ is the measurement error covariance matrix. The contribution functions indicate the variation of the retrieved profile when changing the slant column at a given LOS by a certain amount of molecules per cm^2. The retrieved profile at a specific altitude can be thought of as a weighted average of the true profile with the corresponding averaging kernel.

$$\mathbf{A} = \mathbf{D}\mathbf{K} \tag{8}$$

A change in the real atmospheric profile by a certain amount of molecules per cm^3 in a specific altitude causes a change of a certain amount of molecules per cm^3 in the retrieved profile at all altitudes represented by a function, the averaging kernel for this specific altitude. The vertical resolution of the profile retrieval is determined from the averaging kernels. Rodgers

defined the vertical resolution of a profile retrieval at a specific altitude as the Full Width Half Maximum (FWHM) value of the corresponding averaging kernel [33].

In practice, to calculate the weighting functions needed in the inversion, each layer of the a priori trace gas profile has to be perturbed separately. Using these perturbed profiles the "perturbed" slant columns are calculated by again the radiative transfer model. Thus the elements of the weighting functions matrix can be approximated as follows:

$$K_{i,j} = \frac{dy_i}{dx_j} \approx \frac{\Delta y_i}{\Delta x_j} = \frac{y_i - y_i^p}{x_j - x_j^p} \tag{9}$$

i represents the index over all measurements and j represents the index over all perturbed layers, y_i^p is the slant column calculated with a perturbed profile x_j^p at layer j. After calculating the contribution functions using eq. 7 the averaging kernels can be calculated using eq. 8.

5. Retrieval Error Analysis

The total error of the retrieved profile can be separated into three components. According to Rodgers[33] the total error of the profile retrieval is the difference between the retrieved and the true profile. Due to error propagation the error covariance matrix of the total error can be written as:

$$\mathbf{S}_{tot} = \mathbf{S}_n + \mathbf{S}_m + \mathbf{S}_f \tag{10}$$

$\mathbf{S}_n$ is the a priori error covariance matrix, $\mathbf{S}_m$ is the measurement error covariance matrix or retrieval noise, and $\mathbf{S}_f$ is the forward model error covariance matrix. The last error component will not be considered in this work because the error produced by the forward model SCIATRAN is less than 2% for LOS with tangent heights up to 30 km[34].

The a priori error covariance matrix $\mathbf{S}_n$ can be calculated as:

$$\mathbf{S}_n = \Big(\mathbf{A} - \mathbf{I}\Big)\mathbf{S}_a\Big(\mathbf{A} - \mathbf{I}\Big)^T \tag{11}$$

where $\mathbf{S}_a$ is the error covariance matrix of the a priori profile. Rodgers[33] refers to the a priori error as smoothing error, due to the fact that this covariance matrix $\mathbf{S}_n$ corresponds to portions of profile space the measurements cannot see. In our case those portions are the altitudes in the stratosphere, and small scale variations obscured by the limited altitude resolution of the profile retrieval.

The measurement error covariance matrix $\mathbf{S}_m$ can be calculated as:

$$\mathbf{S}_m = \mathbf{D}\mathbf{S}_\epsilon\mathbf{D}^T \tag{12}$$

where $\mathbf{S}_\epsilon$ is the covariance matrix of the measurement error and $\mathbf{D}$ is the contribution function matrix. The measurement error is due to noise in the measurements propagating into the retrieval. The contribution function matrix maps the measurement error into the profile space.

6. Sensitivity Studies

To assess the amount of profile information contained in AMAX-DOAS measurements, slant columns have been simulated for a number of different scenarios and a retrieval performed using the method described in the previous sections. The results are discussed by evaluating the averaging kernels, weighting functions and retrieval errors. An overview of the different scenarios that have been studied is given in Tab. 1. Briefly, the influence of wavelength, surface spectral reflectance (from now on referred to as albedo), flight altitude and also the choice of LOS and pointing accuracy has been investigated. While the choice of some

parameters (for example standard LOS, flight altitude and wavelength) is based on the set-up and operation of the AMAX-DOAS instrument, the results are valid in general and not restricted to this experiment. Also, the discussion is focused on the case of NO_2 retrieval but can readily be applied to other trace gases taking into account the differences in the absorption cross sections.

As already mentioned above, the trace gas profile was perturbed using a selected altitude grid. This perturbation grid was adapted within the sensitivity studies in order to take into account different vertical resolutions. In this work two perturbation grids are used. The first perturbation grid is used for a flight altitude of 10 km. From 1 to 19 km the step size is 2 km. Between altitudes of 22 and 30 km the step size is also 2 km and above 30 km up to 50 km the step size is 5 km. At a flight altitude of 2 km a second perturbation grid was used. It has a step size of 0.2 km below 4 km, and a step size of 5 km from 10 to 50 km.

For these studies a low aerosol scenario from LOWTRAN[36,37] was chosen, using a visibility in the boundary layer (0 to 2 km) of 23 km, a maritime aerosol type, and 80% humidity. In the free troposphere (2 to 10 km) the visibility is 23 km and the humidity is 80%. In the stratosphere the aerosol loading is that of a background scenario. For all studies, a cloud free scenario was assumed.

The meteorological data used in the radiative transfer model were taken from the 3-dimensional chemical transport model SLIMCAT[38]. A mid-latitude spring scenario is used for these studies. A small arbitrary value of 0.1 ppbv NO_2 was added at the surface and at 1 km altitude. As mentioned above a fixed SZA of 51.6° is used. From the output of the radiative transfer model only data with a 90° relative azimuth angle with respect to the sun was taken into account, assuming there are no horizontal inhomogeneities in the trace gas abundance.

For this retrieval method different LOS are crucial. The following 10 different LOS were assumed in this sensitivity study: 0° (nadir), 60°, 80°, 85°, 88°, 92°, 95°, 100°, 120°, and 180° (zenith).

The sensitivity studies were undertaken for NO_2. To perform the sensitivity studies, appropriate values for the a priori ($\mathbf{S}_a$) and measurement error ($\mathbf{S}_\epsilon$) have to be assumed. Since the measured slant columns will be in the order of 10^{16} molec/cm^2 to $1.5*10^{16}$ molec/cm^2, a standard deviation of 10^{15} molec/cm^2 is a realistic measurement error. A good DOAS instrument is able to measure a differential optical depth as small as $3*10^{-4}$ with a seasonable signal to noise ratio. Using the differential cross section of NO_2 near 500 nm of $2.5*10^{-19}$ cm^2/molecule the smallest slant column measurable with this instrument can be calculated to be $1.2*10^{15}$ molecules/cm^2.

The maximum mixing ratio of the NO_2 profile is in the order of 3 to 4 ppbv. In this case a standard deviation of 1 ppbv as a priori error seems to be reasonable.

7. Results

In Fig. 2 a.) the averaging kernels for scenario 1 are shown. This scenario assumes a flight altitude of 10 km, a wavelength of 350 nm, and an albedo of 0.1. A first look at the averaging kernels reveals a large sensitivity of the profile retrieval near flight altitude. As was discussed above, the averaging kernels at 350 nm cannot be understood by considering only the tangent heights for every LOS. This is because of the limited visibility at 350 nm. There are two distinctive averaging kernels (9 and 11 km) suggesting a very high sensitivity and a vertical resolution of 2 km near the flight altitude between 8 and 12 km. Going further down towards the surface the averaging kernels broaden. In contrast to the 9 km averaging kernel the 1 km averaging kernel has a FWHM value of 3 to 4 km. The changing peak altitudes and FWHM values for the averaging kernels can be understood considering

the limited visibility of the atmosphere in the UV at 350 nm. Good vertical resolution will be achieved if the average light paths through different altitude layers differ strongly. This is the case for the layer close to flight altitude, which is penetrated differently by the individual viewing directions. To understand this pattern of averaging kernels it is necessary to analyze the weighting functions. The section dealing with the retrieval theory described the weighting functions as sensitivity of the measurements as a function of altitude. The maximum of the weighting functions are indicators for the altitude from which most of the information for a given LOS is coming from. The weighting functions for scenario 1 are shown in Fig. 3 a.). The weighting functions for the downward looking LOS peak in different altitudes. This suggests, that different LOS are sensitive to different altitudes.

Above the aircraft the vertical resolution of the averaging kernels decreases. The FWHM of the 11 km averaging kernel is 2 - 3 km, whereas the FWHM value of the 13 km averaging kernel is roughly 3 to 4 km. All averaging kernels above flight altitude peak at 13 km except for the 11 km averaging kernel. The weighting functions of Fig. 3 a.) confirm the information given by the averaging kernels. The sensitivity of the upward looking LOS to altitudes above 13 km is small and does not contain profile information.

As discussed in the previous section the SZA for these sensitivity studies is 51.6°. Two additional SZA (20° and 85°) were tested but results are not presented here as the general behavior of the averaging kernels does not change.

Fig. 4 shows the retrieval errors for different scenarios resulting from the a priori and measurement error described above. The total retrieval error ($S_n + S_m$) is a measure of quality of the retrieval. A small total error indicates a retrieval of high quality.

A comparison with the retrieval error of a profile retrieval using a perturbation grid with 1 km step size (not shown here) reveals that the retrieval error decreases significantly when

the perturbation grid step size is increased. There appears to be sufficient information in the measurements that a 2 km vertical resolution of the retrieved profile seems to be reasonable.

A. Influence of the Wavelength on the Retrieval:

In this investigation two wavelengths were used, one in the UV (350 nm) and one in the visible wavelength region (500 nm). The averaging kernels of scenario 1 [see Fig. 2 a.)] and scenario 2 [see Fig. 2 b.)] are compared. The overall behavior of the averaging kernels at 500 nm is basically the same as at 350 nm.

There are however a few exceptions. The first exception is that the averaging kernels 1 to 9 km split into two categories. In the first category the averaging kernels 7 and 9 km peak at the same altitude suggesting profile information of measurements at 500 nm have a lower vertical resolution than 2 km. In the second category the averaging kernels 1 to 5 km all peak at different altitudes, indicating that profile information of these measurements at 500 nm has a vertical resolution of approximately 2 km. The weighting functions for this scenario are plotted in Fig. 3 b.) and it can be seen that there are no two LOS, that can resolve the layer between flight altitude and 5 km.

The second exception is, that the 1 km averaging kernel has a much larger value compared to the same averaging kernel for 350 nm. This feature suggests a higher sensitivity of the 500 nm measurements in the lower troposphere, as is expected as a result of the reduced importance of Rayleigh scattering at this wavelength.

As can be seen in Fig. 2 b.) the vertical resolution at 500 nm is lower than at 350 nm between 7 and 9 km altitude, but it is higher at an altitude of 5 km. This result is confirmed by the retrieval errors shown in Fig. 4 b.). For 500 nm, the retrieval error between 7 and 9 km is larger than at 350 nm but smaller than that at 350 nm at 5 km.

B. Influence of the Albedo on the Retrieval

To investigate the influence of albedo or surface spectral reflectance, the averaging kernels for albedos of 0.1 and 0.9 respectively are considered for the 2 wavelengths (350 and 500 nm). For scenario 4 at 500 nm [see Fig. 2 d.)] and an albedo of 0.9, there is no significant change compared to scenario 2 at 500 nm and an albedo of 0.1. However, in the UV at 350 nm, the 1 km averaging kernel increases by almost a factor of 2 [see Fig. 2 c.)]. The averaging kernels for altitudes above 1 km do not change when the albedo is changed from 0.1 to 0.9. The same holds for the averaging kernels above the aircraft. This can be explained by taking into account the enhancement of multiple scattering as a result of the larger number of reflected photons at the surface in the UV wavelength region. The enhanced multiple scattering is limited to the lower altitudes (below 1 km), because multiple scattering is occurring and most likely in parts of the atmosphere having a higher density. The overall result of this study is that large albedo will increase the sensitivity of UV measurements in the surface layer but apart from that there is little influence on the profile information of the measurements.

C. Influence of Additional Lines of Sight on the Retrieval:

To investigate the usefulness of having different LOS [see Fig. 2 f.); scenario 6] the calculations for two additional LOS (89° and 91°) were included at 500 nm compared to scenario 2 [see Fig. 2 b.)]. For scenario 6 the averaging kernels 7 and 9 km below the aircraft peak in different altitudes compared to those in scenario 2. The weighting functions for this scenario [Fig. 3 d.)] explains this behavior. For the 89° LOS, the retrieval obtains information exclusively from the altitudes near 9 km, because the majority of the absorption signal originates from these altitudes. The 88° LOS weighting function is the same as in scenario 2. Therefore, as a result of the additional LOS, additional profile information about higher altitudes

is gathered. For 350 nm [see. Fig. 3 c.)] there is no difference in the weighting functions of the 88°, and the 89° LOS. Thus no increase in the vertical resolution is observed. The fact that the additional LOS do not increase the profile resolution at 350 nm results from the limited visibility at 350 nm. Above the aircraft the averaging kernels do not change compared to scenario 1.

Fig. 3 c.) shows that the vertical resolution at 500 nm can be improved when using additional LOS at 89° and 91°. Analysis of the retrieval errors in Fig. 4 c.) confirms the improvement of the resolution at 500 nm due to the smaller retrieval error compared to scenario 2. However, in real applications, the pointing accuracy needed for these LOS is difficult to achieve because of the intrinsic pitch and roll of an aircraft in flight.

D. Influence of the Flight Altitude on the Retrieval

In this part of the study calculations for a flight altitude of 2 km are compared to those for 10 km flight altitude. Again, two cases have to be considered. The first case is the scenario 7 calculated for a wavelength of 350 nm, the second one is calculated for a wavelength of 500 nm. As can be seen in Fig. 5 a.) and c.) for scenario 7, the averaging kernels calculated for this flight altitude do not peak as distinctively as they did for the 10 km flight altitude. This is to be expected given the vertical resolution of 2 km that could be achieved at 10 km. Above and below the flight altitude, the peak values of the averaging kernels are decreasing rapidly. This fact and a study of the retrieval error (not shown) suggest that the measurement at 2 km flight altitude is not containing much profile information. In summary measurements at 2 km yield an in-situ measurement at flight altitude to the columns below and above the aircraft. The averaging kernels above the aircraft contain less profile information compared to measurements taken at 10 km flight altitude in the UV.

The second case is the scenario 8 calculated for a wavelength of 500 nm. As can be seen in

Fig. 5 b.) and d.), the averaging kernels are nearly identical to the UV case with the exception that the 0.2 km averaging kernel has larger values. Even the difference of averaging kernels between the two wavelengths is small. This is because the distances from the aircraft to the surface for almost all LOS for both wavelengths are within the visibility range of the model atmosphere for both the visible and the UV. The main result of this study is that only 2 layers beneath the aircraft are resolved for this flight altitude, namely from 0 to 1 km and from 1 to 2 km. Above the aircraft the retrievable number of layers is only two, from 2 to 2.5 km and above 2.5 km.

E. What is the optimum LOS setup?

This question has two parts. The first is addressing the optimum number of LOS required, when retrieving a profile with a certain resolution. Rodgers deals with this part of the question by the use of prior constraints. To make the inversion problem well-posed 'a discrete representation with fewer parameters than the number of degrees of freedom of the measurements', as required by the maximum a posteriori method is needed ([33], chapter 10). For our example this translates to: if the retrieved profile below the aircraft has 5 points, at least 5 measurements (downward looking LOS) are needed to make the problem well-posed. The second part of the question deals with the selection of LOS for a specific setup. This can be answered by selecting the LOS in such a way that for each layer in the retrieval grid one limb measurement is taken that has the appropriate tangent height. For the retrieval grid of 0 km, 1 km, 3 km, ..., 9 km the according LOS would be: 86.8°, 87.0°, 87.3°, 87.7°, 88.2°, and 89.0°.

In practice this approach in not very useful because the required pointing accuracy of 0.2° is difficult to realize. Therefore a downsized version of this approach will be tested. Instead of 18 LOS required for all tangent heights from 0 to 9 km only 12 LOS will be used. This

scenario is realized by using the LOS 0°, 80°, 85°, 88°, 89°, 91°, 92°, 95°, 100°, and 180° plus the LOS 87° and 93°. The comparison of the 18 LOS study to the 12 LOS study (not shown here) reveals a difference in averaging kernel peak values of less than 10%. This is a small change compared to the 60% increase in the 3 km averaging kernel peak value between the additional LOS (scenario 6) and the 12 LOS study (scenario 10) at 500 nm [see Fig. 2 f.) and Fig. 6 b.)]. From this we conclude, that no further information is gathered in going from 12 to 18 LOS. At 350 nm there is practically no difference between the 10 LOS setup and the 12 LOS setup [see Fig. 2 e.) and Fig. 6 a.)]. The 18 LOS setup (not shown here) does not increase the averaging kernel peak values. At 350 nm, the 10 LOS setup is already the LOS setup with the best performance. For 500 nm the LOS setup with the best performance is the setup with 18 LOS but for practical reasons the 12 LOS setup is as good as the 18 LOS setup. The retrieval error for the 12 LOS study at 500 nm [see. Fig. 4 d.)] supports the better performance of the 10 LOS.

F. Influence of the Pointing Accuracy on the Retrieval

The last part of this investigation deals with the pointing accuracy of the LOS. To test the influence of the pointing accuracy on the retrieval, the retrieval errors were calculated for a profile retrieval of the 12 LOS study and pointing error was added to each LOS. To characterize the decrease in retrieval quality, the ratio of the retrieval error with and without pointing error was calculated (see Fig. 7). A pointing error of less than 1° does not change the retrieval error significantly at 350 nm as shown in Fig. 7 a.). The largest relative changes occur at altitudes with small retrieval errors, and therefore the absolute retrieval quality is not decreased significantly. At 500 nm a pointing accuracy of better than 1° is very important as can be seen in Fig. 7 b.) to d.). The same retrieval quality as for 350 nm is achieved, when a pointing pointing accuracy of better than 0.1° is assumed. For

real flights the pointing accuracy for all LOS is known a posteriori as good as 0.01°.

8. Conclusions

Sensitivity studies have been performed to determine the amount of profile information contained in airborne UV/vis skylight absorption measurements. The result of this work is that there is indeed valuable profile information in airborne multi axis UV/vis skylight absorption measurements. The vertical resolution of the profile retrieval depends on the LOS setup, the flight altitude, and the wavelength. Airborne multiaxis measurements have an excellent sensitivity in the troposphere and upper troposphere/lower stratosphere. Tab. 2 shows how much profile information each scenario yields.

The investigation of the influence of the wavelength at 350 nm on the the retrieval indicates that measurements in the UV contain more profile information than measurements at 500 nm. For 350 nm, a profile resolution of 2 km below the aircraft is predicted up to 14 km altitude with one column being retrieved above 14 km altitude. At 500 nm, the resolution is slightly lower: 2 km from 0 to 6 km altitude, 3 to 4 km resolution from 6 to 10 km altitude, 2 km resolution from 10 to 14 km altitude, and a column above 14 km altitude.

When comparing the averaging kernels for high and low albedo, it turns out that the differences are small at both wavelengths with exception of the UV averaging kernel nearest to the surface. Albedo is therefore not a critical parameter for the retrieval as calculated.

Additional lines of sight near the horizon will improve the profile resolution near flight altitude at 500 nm whereas the profile resolution at 350 nm remains basically the same (not shown). This can be seen by comparing figures 3 b.) and 3 c.) and figures 2 b.) and 2 f.). With additional lines of sight at 500 nm the resolution of the retrieved profile will be as good as or better than the resolution of scenario 1. However, in practice it is difficult to achieve the necessary pointing accuracy close to the horizon on a moving aircraft and the

potential improvement might not be possible in practice.

The main result obtained in the study of the influence of the flight altitude is that at lower altitudes little profile information can be retrieved from the measurements for either wavelength. The reason is, that most of the profile information comes from the downward looking limb LOS. For lower flight altitudes the number of LOS in limb mode decreases rapidly assuming a fixed LOS setup. Still, near flight altitude enhanced sensitivity is achieved adding some vertical resolution to the measurements. In practice, flying at different altitudes does provide profile information since these studies have shown that the best profile information can be extracted from the flight altitude region.

The study to analyze the question addressing the issue of the best LOS setup indicates the 10 LOS setup [0° (nadir), 80°, 85°, 88°, 89°, 91°, 92°, 95°, 100°, and 180° (zenith)] as a reasonable optimum setup at 350 nm, where at 500 nm the optimum is with 12 LOS [0° (nadir), 80°, 85°, 87°, 88°, 89°, 91°, 92°, 93°, 95°, 100°, and 180° (zenith)].

Concerning the requirements on pointing accuracy, it turns out that a pointing accuracy of 1° is sufficient for measurements at 350 nm but a pointing accuracy of 0.1° is required for measurements at 500 nm.

For practical applications, clouds, horizontal inhomogeneities, and aerosols will introduce further uncertainties and reduce the achievable vertical resolution of the retrieved profile. The combination of two or even more wavelengths contains a large optimization potential, since it is shown that the same LOS using different wavelengths is sensitive to different altitudes of the profile. The sensitivity studies have also shown that these measurements are most sensitive to profile information close to flight altitude. Therefore combination of measurements at different altitudes, and possibly also at different SZA has the potential of adding profile information, further improving the theoretical vertical resolution. Overall

this sensitivity study demonstrates the potential of AMAX-DOAS measurements to provide height resolved information on a number of relevant species in the troposphere and the important UTLS region using a relatively simple remote sensing instrument on an airborne platform.

9. Acknowledgements

Part of this work was funded by the "SCIAMACHY Validations Programm" (Förderkennzeichen 50EE0023) by means of the German Ministry of Sciences (BMBF) and the University of Bremen. We would like to thank Kathy Preston and Howard Roscoe for providing the computer code this work is based on. Last but not least we would like to thank Martin Chipperfield for providing the data of the 3-D SLIMCAT model output. The authors would like to thank two anonymous reviewers for helpful comments and suggestions.

References

1. A. W. Brewer, C. T. McElroy, and J. B. Kerr, "Nitrogen Dioxide Concentrations in the atmosphere", Nature, **246 (5429)**, 129-133, (1973)
2. J. F. Noxon, "Nitrogen dioxide in the stratosphere and troposphere measured by ground-based absorption spectroscopy", Science, **189**, 547-549, (1975)
3. R. L. McKenzi and P. V. Johnston, "Seasonal variations in stratospheric NO_2 at 45°S", Geophys. Res. Lett., **9**, 1255-1258, (1982)
4. J. P. Pommereau and F. Goutail, "O_3 and NO_2 Ground-Based Measurements by Visible Spectrometry during Arctic Winter and Spring 1988", Geophys. Res. Lett., **15**, 891-894, (1988)
5. S. Solomon, A. L. Schmeltekopf, and R. W. Sanders, "On the interpretation of zenith sky absorption measurements", J. Geophys. Res., **92**, 8311-8319, (1987)

6. U. Platt, Differential optical absorption spectroscopy (DOAS), in Air Monitoring by Spectroscopic Techniques, Chem. Anal. Ser., vol. 127, edited by M. W. Sigrist, pp. 27–84, John Wiley, New York, 1994.

7. J. F. Noxon, E. C. Whipple Jr., and R. S. Hyde, "Stratospheric NO_2: 1. Observational method and behavior at mid-latitudes", J. Geophys. Res., **84**, 5047-5065, (1979)

8. R. L. McKenzi, P. V. Johnston, C. T. McElroy, J. B. Kerr, and S. Solomon, "Altitude distributions of stratospheric constituents from ground-based measurements at twilight", J. Geophys. Res., **96**, 15499-15511, (1991)

9. K. E. Preston, "The Retrieval of NO_2 vertical profiles from ground-based Twilight UV-visible measurements", Ph.D. Thesis, Pembroke College, Cambridge, (1995)

10. K. E. Preston, R. L. Jones, and H. K. Roscoe, "Retrieval of NO_2 vertical profiles from ground-based UV-visible measurements: Method and validation", J. Geophys. Res., **102**, 19089-19097, (1997)

11. L. A. Barrie, J. W. Bottenheimer, R. C. Schnell, P. J. Crutzen, and R. A. Rasmussen, "Ozone destruction and photochemical reactions at polar sunrise in the lower Arctic atmosphere", Nature, **334**, 138-141, (1988)

12. M. Hausmann and U. Platt, "Spectroscopic measurements of bromine oxide in the high Arctic during Polar Sunrise Experiment 1992", J. Geophys. Res., **99**, 25399-25413, (1994)

13. A. Richter, F. Wittrock, M. Eisinger, and J. P. Burrows, "GOME Observations of Tropospheric BrO in Northern Hemispheric Spring and Summer 1997", Geophys. Res. Lett., **25**, 2683-2686, (1998)

14. T. Wagner and U. Platt, "Satellite mapping of enhanced BrO concentrations in the troposphere", Nature, **395**, 486-490, (1998)

15. C. T. McElroy, C. A. McLinden, and J. C. McConnell, "Evidence for bromine monoxide in the free troposphere during the Arctic polar sunrise", Nature, **397**, 338-341, (1999)

16. T. Wagner, C. Leue, M. Wenig, K. Pfeilsticker, U. Platt, "Spatial and temporal distribution of enhanced boundary layer BrO concentrations measured by the GOME instrument aboard ERS-2", J. Geophys. Res., **106**, 24225-24236, (2001)

17. M. Van Roozendael, A. Richter, T. Wagner, I. Pundt, D. W. Arlander, J. P. Burrows, M. Chipperfield, C. Fayt, P. V. Johnston, J.-C. Lambert, K. Kreher, K. Pfeilsticker, U. Platt, J.-P. Pommereau, B.-M. Sinnhuber, K. K. Tornkvist, and F. Wittrock, "Intercomparison of BrO Measurements From ERS-2 GOME, Ground-Based and Balloon Platforms", Adv. Space Res., **29**, 1661-1666, (2002)

18. A. Wahner, R. O. Jakoubek, G. H. Mount, A. R. Ravishankara, and A. L. Schmeltekopf, "Remote Sensing Observations of Nighttime OClO Column During the Airborne Antarctic Ozone Experiment, September 8, 1987", J.Geophys. Res., **94**, 11405-11411, (1989)

19. A. Wahner, R. O. Jakoubek, G. H. Mount, A. R. Ravishankara, and A. L. Schmeltekopf, "Remote Sensing Observations of Daytime Column NO_2 During the Airborne Antarctic Ozone Experiment, August 22 to October 2, 1987", J.Geophys. Res., **94**, 16619-16632, (1989)

20. A. Wahner, J. Callies, H.-P. Dorn, U. Platt, and C. Schiller, "Near UV Atmospheric Absorption Measurements of Column Abundances During Airborne Arctic Stratospheric Expedition, January-February 1989: Technique and NO_2 Observations", Geophys. Res. Lett., **17**, 497-500, (1990)

21. A. Wahner, J. Callies, H.-P. Dorn, U. Platt, and C. Schiller, "Near UV Atmospheric Absorption Measurements of Column Abundances During Airborne Arctic Stratospheric

Expedition, January-February 1989: 3. BrO Observations", Geophys. Res. Lett., **17**, 517-520, (1990)

22. C. Schiller, A. Wahner, H.-P. Dorn, U. Platt, J. Callies, and D. H. Ehhalt, "Near UV Atmospheric Absorption Measurements of Column Abundances During Airborne Arctic Stratospheric Expedition, January-February 1989: 2. OClO Observations", Geophys. Res. Lett., **17**, 501-504, (1990)
23. R. Brandtjen, T. Klüpfel, D. Perner, and B. M. Knudsen, "Airborne measurements during the European Arctic Stratospheric Ozone Experiment: Observation of OClO", Geophys. Res. Lett., **21**, 1363-1366, (1994)
24. K. Pfeilsticker and U. Platt, "Airborne measurements during the European Arctic Stratospheric Ozone Experiment: Observation of O_3 and NO_2", Geophys. Res. Lett., **21**, 1375-1378, (1994)
25. F. Erle, A.Grendel, D. Perner, U. Platt, and K. Pfeilsticker, "Evidence of heterogeneous bromine chemistry on cold stratospheric sulphate aerosols", Geophys. Res. Lett., **25**, 4329-4332, (1998)
26. M. L. Melamed, S. Solomon, J. S. Daniel, A. O. Langford, R. W. Portmann, T. B. Ryerson, D. K. Nicks, Jr. and S. A. McKeen, "Measuring reactive nitrogen emissions from point sources using visible spectroscopy from aircraft", J. Environ. Monit., **5**, 29-34, (2003)
27. A. Petritoli, F. Ravegnani, G. Giovanelli, D. Bortoli, U. Bonaf, I. Kostadinov, A. Oulanovsky, "Off-Axis Measurements of Atmospheric Trace Gases by Use of an Airborne Ultraviolet-Visible Spectrometer", Applied Optics, **27**, 5593-5599, (2002)
28. T. Wagner, M. Bruns, J.P. Burrows, S. Fietkau, F. Finocchi, K.-P. Heue, G. Hönninger, U. Platt, I. Pundt, A. Richter, R. Rollenbeck, C. von Friedeburg, F. Wittrock, P. Xie,

"The AMAX-DOAS instrument and its application for SCIAMACHY validation", Proceedings of the 15th ESA Symposium on European Rocket and Balloon Programmes and Related Research (ESA SP-471, August 2001), Biarritz, France, 28-31 May, (2001)

29. G. Hönninger and U. Platt, "The Role of BrO and its Vertical Distribution during Surface Ozone Depletion at Alert", Atmos. Environ., **36**, 2481-2489, (2002)

30. F. Wittrock, H. Oetjen, A. Richter, S. Fietkau, T. Medeke, A. Rozanov, and J. P. Burrows, MAX-DOAS measurements of atmospheric trace gases in Ny-Ålesund, Atmos. Chem. Phys. Discuss., **3**, 6109–6145, (2003)

31. C. D. Rodgers, "Retrieval of atmospheric temperature and composition from remote measurements of thermal radiation", Rev. Geophys., **14**, 609-624, (1976)

32. C. D. Rodgers, "Characterization and error analysis of profiles retrieved from remote sounding measurements", J. Geophys. Res., **95, D5**, 5587-5595, (1990)

33. C. D. Rodgers, *Inverse Methods for atmospheric sounding: Theory and Practice*, Series on Atmospheric, Oceanic and Planetary Physics, Vol. 2, (World Scientific Publishing, London, 2000)

34. A. Rozanov, V. Rozanov and J. P. Burrows, "A numerical radiative transfer model for a spherical planetary atmosphere: combined differential integral approach involving the Picard iterative approximation", J. Quant. Spectrosc. Radiat. Transfer, **69**, 491-512, (2001)

35. L. C. Marquard, T. Wagner, and U. Platt, "Improved air mass factor concepts for scattered radiation differential optical absorption spectroscopy of atmospheric Species", J. Geophys. Res., **105**, 1315-1327, (2000)

36. E. P. Shettle and R. W. Fenn, "Models of the aerosols of the lower atmosphere and the effects of humidity variations on their optical properties", Tech. rep., AFGL-TR-

79-0214, Project 7670, Air Force Geoph. Lab., Hanscom AFB, MA, (1979)

37. F. X. Kneizys, E. P. Shettle, L. W. Abreu , J. H. Chetwynd, G. P. Anderson, W. O. Gallery, J. E. A. Selby, and S. A. Clough, Üsers Guide to LOWTRAN 7", Tech. rep., AFGL-TR-88-0177, (NTIS AD A206773), Air Force Geophysics Laboratory AFGL, Hanscom AFB, MA, (1986)

38. M. Chipperfield, "Multiannual simulations with a three-dimensional chemical transport model", J. Geophys. Res., **104**, 1781-1805, (1999)

39. H. Bovensmann, J. P. Burrows, M. Buchwitz, J. Frerick, S. Nol, V. V. Rozanov, K. V. Chance, and A. H. P. Goede, "SCIAMACHY - Mission objectives and measurement modes", J. Atmos. Sci., **56**, (2), 127-150, (1999)

List of Figure Captions

Fig. 1: This plot shows the light paths observed by an airborne UV/vis skylight absorption spectrometer (a) compared to the light paths observed by a ground-based UV/vis zenith sky absorption spectrometer (b). The displayed light paths indicate the most probable light paths. In reality the light observed at a specific LOS originates from a variety of different light paths as a result of multiple scattering.

Fig. 2: Averaging kernels for a.) scenario 1, b.) scenario 2, c.) scenario 3, d.) scenario 4, and e.) scenario 6.

Fig. 3: Weighting functions for a.) scenario 1, b.) scenario 2, and c.) scenario 6. The NO_2 profile is anticipated for mid-latitudes on the northern hemisphere in March at 51.6° SZA. Each weighting function corresponds to a different LOS. The magnitude of the weighting functions is small at the surface and above 15 km, revealing that the slant columns are not very sensitive to NO_2 in these regions.

Fig. 4: Retrieval errors for a.) scenario 1, b.) scenario 2, c.) scenario 6, and d.) scenario 10. S_n is the a priori error, S_m is the measurement error or retrieval noise, and $S_n + S_m$ is the total error of the profile retrieval.

Fig. 5: Averaging kernels for scenarios 6 [a.) and c.)] and 7 [b.) and d.)].

Fig. 6: Averaging kernels for a.) scenario 9 and b.) scenario 10.

Fig. 7: Pointing accuracy: a.) pointing error of -1° for scenario 9, b.) pointing error of -0.5° for scenario 10, c.) pointing error of -0.25° for scenario 10, and d.) pointing error of -0.1° for scenario 10. To characterize the decrease in quality of the retrieval the ratio of the retrieval error with and without pointing error was plotted.

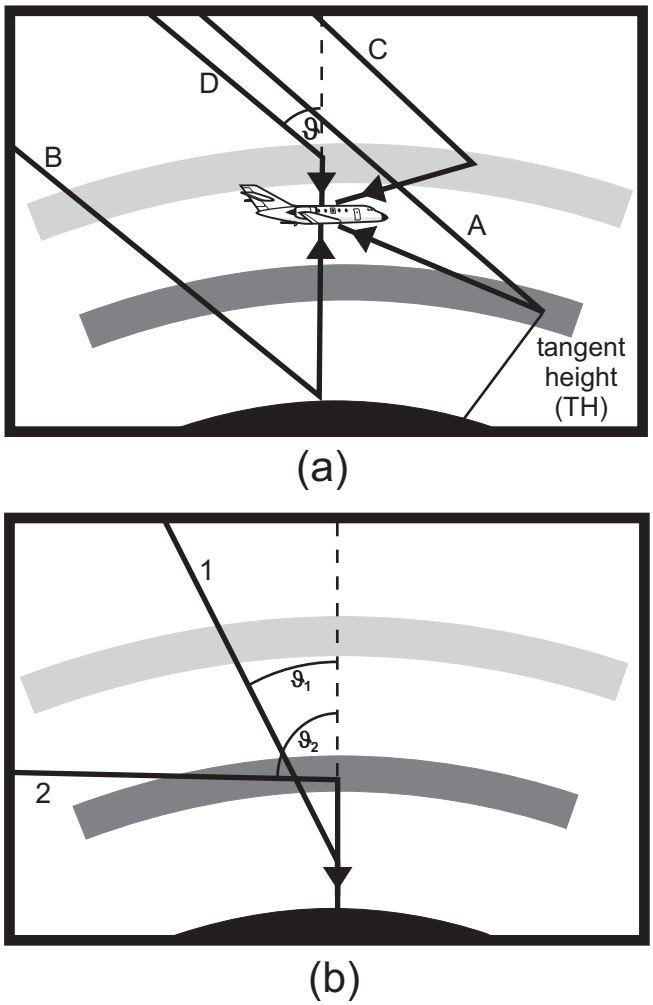

Fig. 1. This plot shows the light paths observed by an airborne UV/vis skylight absorption spectrometer (a) compared to the light paths observed by a ground-based UV/vis zenith sky absorption spectrometer (b). The displayed light paths indicate the most probable light paths. In reality the light observed at a specific LOS originates from a variety of different light paths as a result of multiple scattering.

Table 1. Scenarios for the sensitivity studies.

scenario	albedo	λ [nm]	flight altitude [km]
1	0.1	350	10
2	0.1	500	10
3	0.9	350	10
4	0.9	500	10
5♮	0.1	350	10
6♮	0.1	500	10
7♭	0.1	350	2
8♭	0.1	500	2
9♢	0.1	350	10
10♢	0.1	500	10

♮ For these scenarios the observations of 60° and 120° were replaced by the these of the LOS 89° and 91°.

♭ For these scenarios the step size of the grid is 0.2 km (0-4 km) and 5 km (10 - 50 km). For all other scenarios the step size of the grid is 2 km (1-19 km,22 -30 km) and 5 km (30 - 50 km).

♢ For these scenarios 12 LOS were used: the LOS of scenarios 5 and 6 plus the LOS 87° and 93°.

Table 2. Vertical profile resolution of the considered sensitivity studies.

	flight		layers above	layers below
scenario	altitude [km]	λ [nm]	aircraft	aircraft
1	10	350	5	3
2	10	500	4	3
5♮	10	350	5	3
6♮	10	500	5	3
7	2	350	2	2
8	2	500	2	2
9♭	10	350	5	3
10♭	10	500	5	3

♮ For these scenarios the 60° and 120° were exchanged by the additional LOS 89° and 91°.

♭ For these scenarios 12 LOS were used: the LOS of scenarios 5 and 6 plus the LOS 87° and 93°.

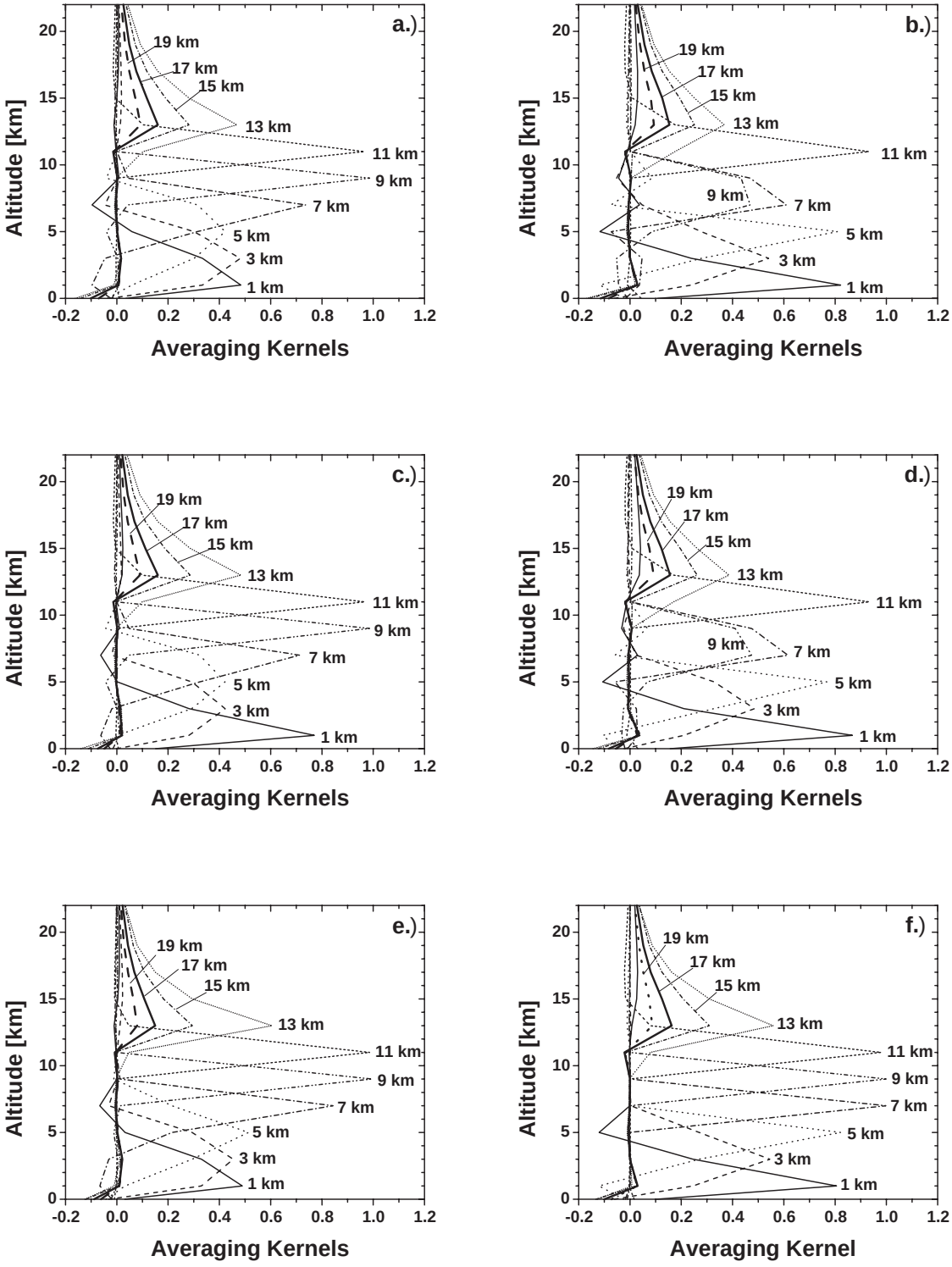

Fig. 2. Averaging kernels for a.) scenario 1, b.) scenario 2, c.) scenario 3, d.) scenario 4, e.) scenario 5, and f.) scenario 6.

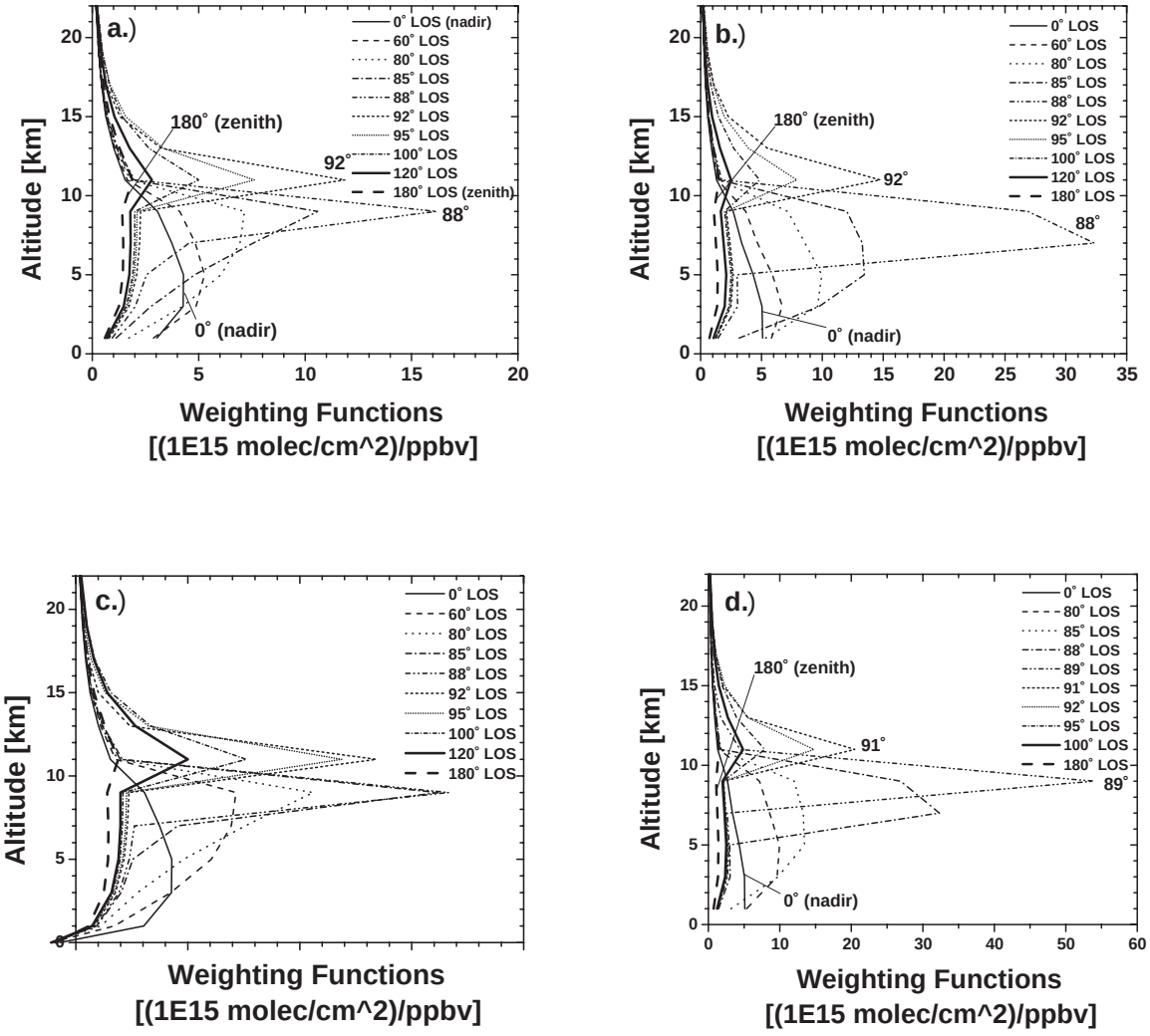

Fig. 3. Weighting functions for a.) scenario 1, b.) scenario 2, c.) scenario 5, and d.) scenario 6. The NO_2 profile is anticipated for mid-latitudes on the northern hemisphere in March at 51.6° SZA. Each weighting function corresponds to a different LOS. The magnitude of the weighting functions is small at the surface and above 15 km, revealing that the slant columns are not very sensitive to NO_2 in these regions.

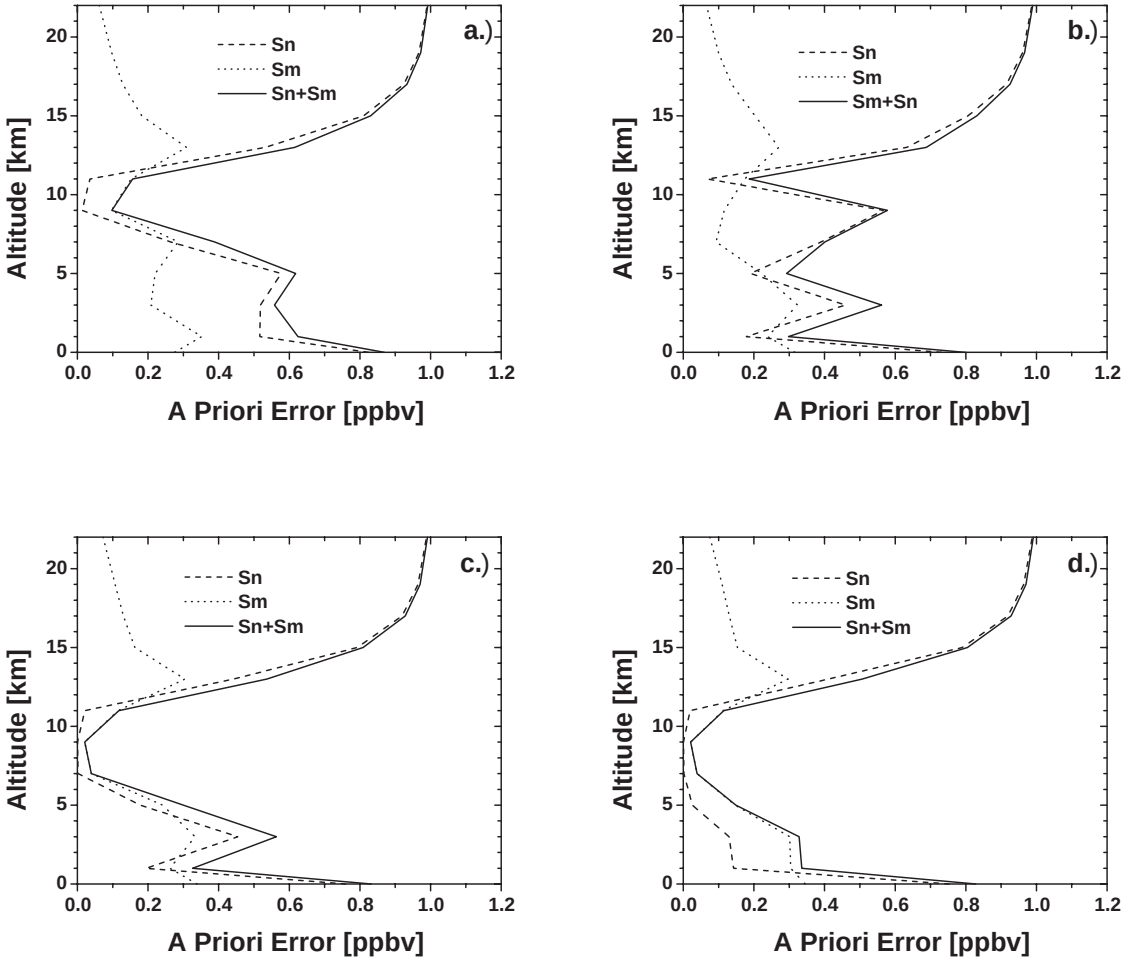

Fig. 4. Retrieval errors for a.) scenario 1, b.) scenario 2, c.) scenario 6, and d.) scenario 10. S_n is the a priori error, S_m is the measurement error or retrieval noise, and $S_n + S_m$ is the total error of the profile retrieval.

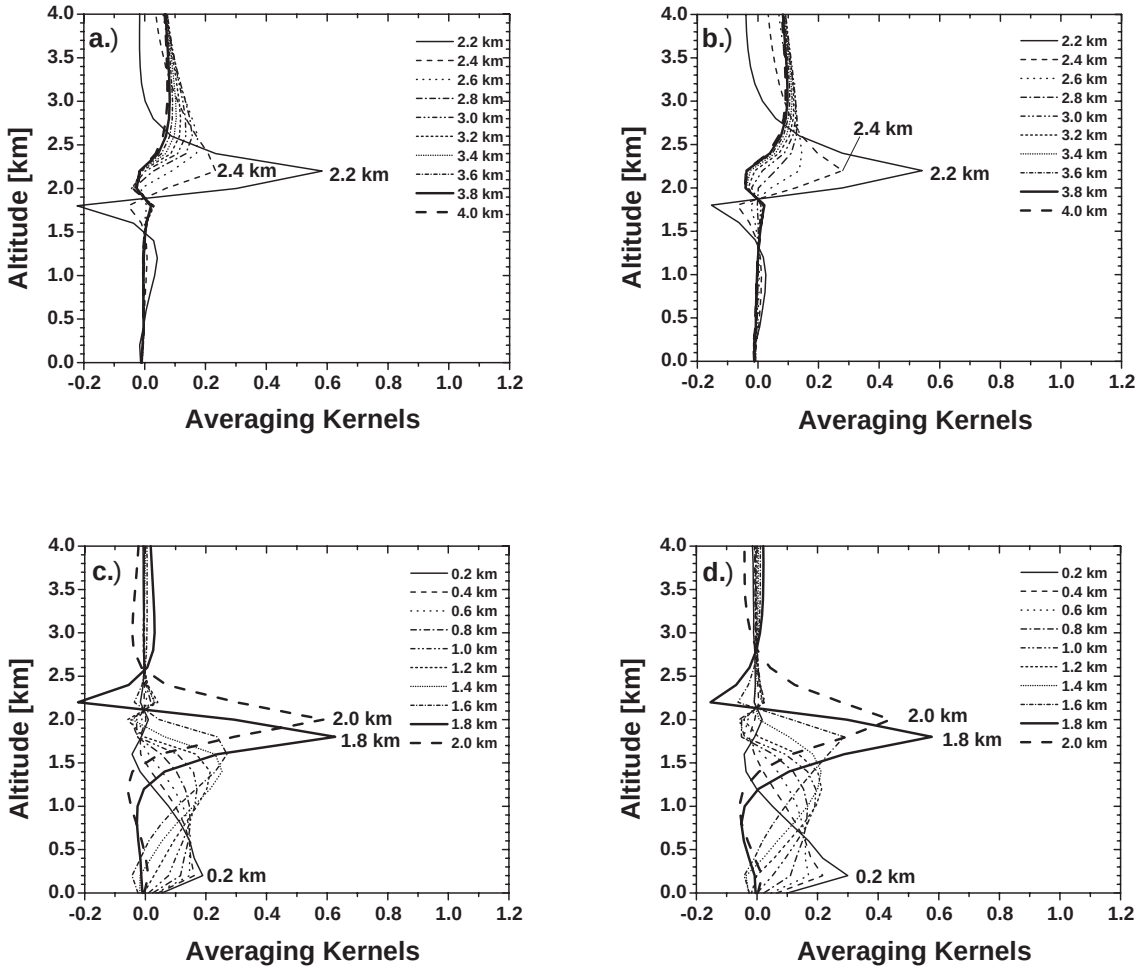

Fig. 5. Averaging kernels for scenario 7 [a.) and c.)] and for scenario 8 [b.) and d.)].

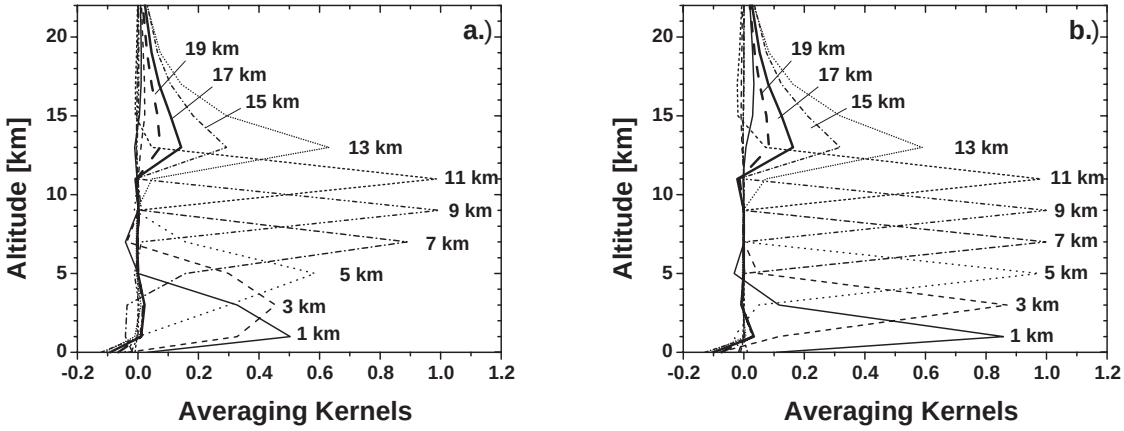

Fig. 6. Averaging kernels for a.) scenario 9 and b.) scenario 10.

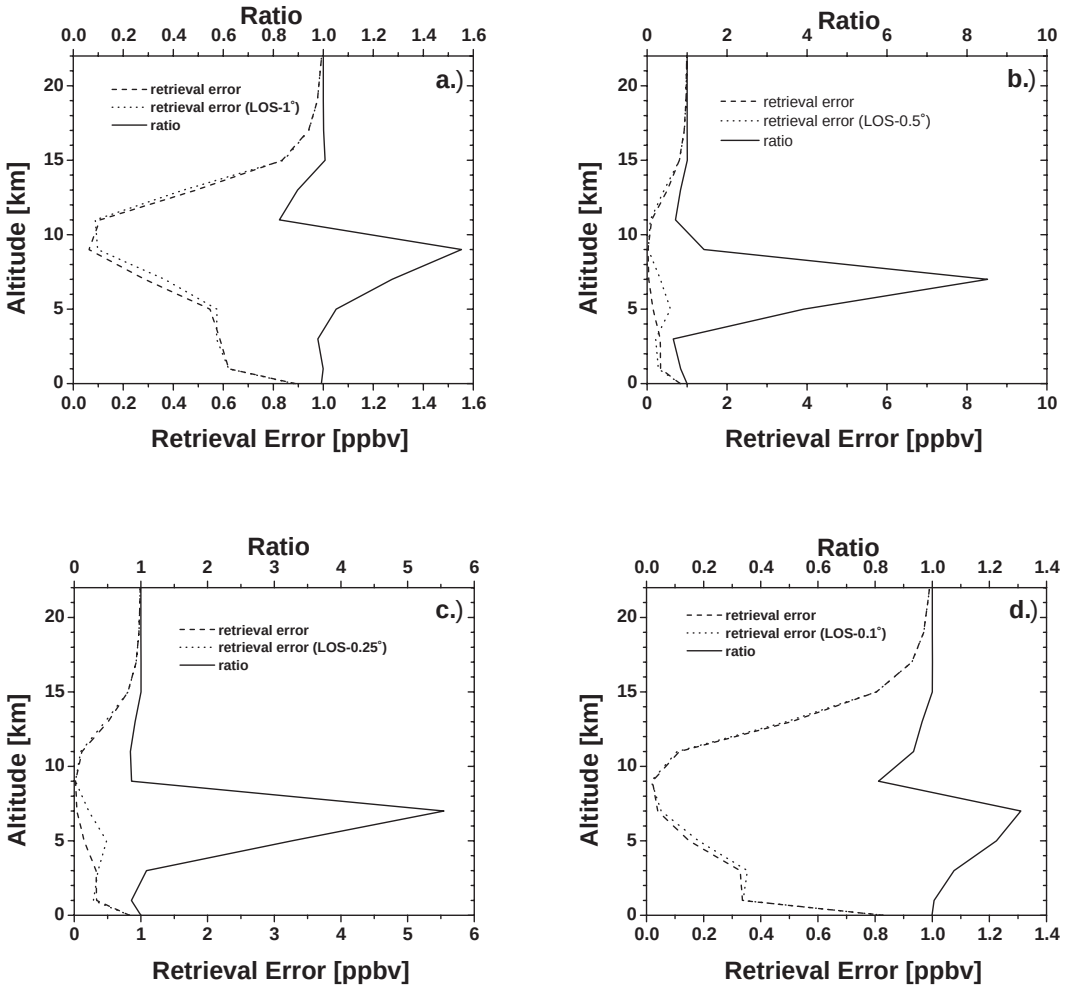

Fig. 7. Pointing accuracy: a.) pointing error of -1° for scenario 9, b.) pointing error of -0.5° for scenario 10, c.) pointing error of -0.25° for scenario 10, and d.) pointing error of -0.1° for scenario 10. To characterize the decrease in quality of the retrieval the ratio of the retrieval error with and without pointing error was plotted.